J. Phys. B: At. Mol. Opt. Phys. 27 (1994) 3687–3694. Printed in the UK

He^{2+} formation in collisions between fast He^{+} ions

J G Murphy, K F Dunn and H B Gilbody

Department of Pure and Applied Physics, The Queen's University of Belfast, Belfast, UK

Received 28 February 1994

Abstract. A fast intersecting beam technique similar to that used previously in this laboratory has been used to study He^{2+} formation in He^{+}–He^{+} collisions at CM energies within the range 54–229 keV. Absolute total cross sections for He^{2+} formation have been determined and the separate contributions from charge transfer and ionization have also been obtained. The process of simultaneous electron loss by both He^{+} ions has been shown to be relatively unlikely even at the highest energies considered. The measurements usefully extend previous lower energy data and, while agreement with these is generally satisfactory, some discrepancies have also been noted. The energy dependence of the measured cross sections for charge transfer indicate an unusually broad structure in general accord with one theoretical prediction. Comparisons with a number of theoretical descriptions have been made for both charge transfer and ionization.

1. Introduction

Over the past decade, experimental studies based on the fast intersecting beam technique have provided detailed information on electron capture and ionization in collisions between positive ions (cf Gilbody 1982, Salzborn 1989). Interest in cross sections for collisions involving helium ions stems from the need for accurate modelling of high temperature fusion plasmas. Such data can also provide a valuable assessment of the range of validity of current theoretic descriptions of particular collision processes.

In the present work, an intersecting beam technique developed previously in this laboratory, has been adapted to carry out studies of He^{+}–He^{+} collisions at CM energies in the range 54–229 keV. The processes we consider are charge transfer

$$He^{+} + He^{+} \rightarrow He(\Sigma) + He^{2+} \qquad (1)$$

(where Σ denotes all final bound states of He) with cross section ${}_{11}\sigma_{02}$, ionization

$$He^{+} + He^{+} \rightarrow He^{+} + He^{2} + e \qquad (2)$$

with cross section ${}_{11}\sigma_{12}$ and the process of simultaneous electron loss by both He^{+} ions

$$He^{+} + He^{+} \rightarrow He^{2+} + He^{2+} + 2e \qquad (3)$$

with cross section ${}_{11}\sigma_{22}$. We have measured total cross sections $\sigma(He^{2+})$ for He^{2+} production from all three processes. We have also carried out separate measurements of cross sections for (1) and (3) so that ionization cross sections for (2) could then be

0953-4075/94/163687+08$19.50

obtained from the expression

$$_{11}\sigma_{12} = \sigma(\mathrm{He}^{2+}) - {}_{11}\sigma_{02} - {}_{11}\sigma_{22}. \tag{4}$$

Previous measurements of $\sigma(\mathrm{He}^{2+})$ and $_{11}\sigma_{02}$ have been carried out by Peart *et al* (1983) within the CM energy range 14–58 keV. In addition Melchert *et al* (1987a, b) have measured $_{11}\sigma_{02}$ and $\sigma(\mathrm{He}^{2+})$ in the respective CM energy ranges 7–112 keV and 11–113 keV. The present results take account of the three possible He^{2+} production mechanisms and provide a useful extension of the previous measurements to higher energies where theoretical predictions can now be tested.

2. Experimental approach

2.1. General description

The apparatus and measuring procedure was basically similar to that described in our previous work (cf Neill *et al* 1982) and, while some important improvements have been made, only the main features need be described here. A schematic diagram of the intersecting beam arrangement used in the present work is shown in figure 1.

The primary He^+ beam from a van de Graaff accelerator of energy adjustable within the range 100–450 keV was momentum analysed and entered the ultra-high vacuum collision chamber via the canal C1. The target He^+ ion beam from a second accelerator

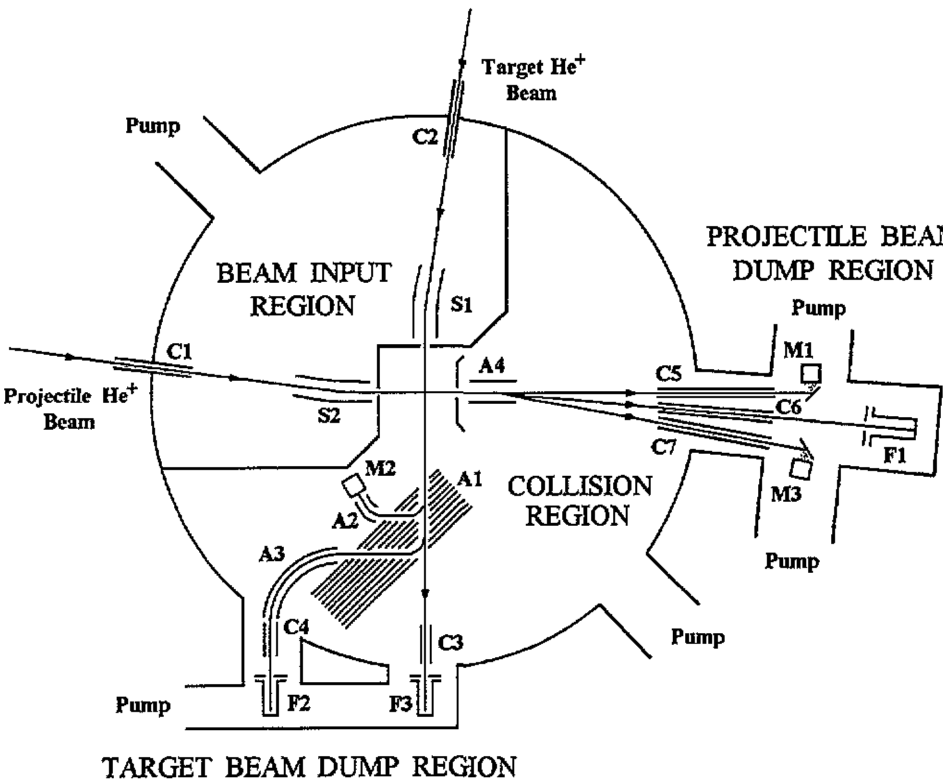

Figure 1. Simplified schematic diagram of the intersecting beam apparatus.

was also momentum analysed and entered the collision chamber via a canal C2. The target beam energy could be adjusted within the range 6–14 keV. Both beams were steered by the electrostatic deflection plates S1 and S2 and intersected at 90° at the centre of the collision chamber where the pressure was maintained at about 2×10^{-10} mbar. This was facilitated by the provision of differential pumping (figure 1) for the beam input region and for both the projectile and target beam 'dump' regions. Having regard to the beam transit times from the ion sources in the two accelerators and the electric fields applied within the beamlines, which would quench any metastable $He^+(2s)$ ions present, the excited state population of the He^+ ion beams at the intersection point was considered to be negligible.

After collision with the projectile beam, the He^{2+} ions formed in the target beam were separated from the much larger He^+ component by a two stage electrostatic analyser A1 and A2 and counted by the particle multiplier M2 (Johnston Type MM1-1SG). This could be calibrated *in situ* with a low intensity He^{2+} beam which could be measured as a current to a screened Faraday cup F3 by a sensitive electrometer. The He^+ component of the target beam was selected by the analysers A1 and A3 and recorded as a current to F2.

Beyond the beam intersection region, the content of the fast projectile beam was analysed by the electrostatic deflection plates A4 so that the He^+, He^{2+} and He components could then be separately recorded. The He and He^{2+} components impinged upon negatively biased plates and the resulting secondary electrons were counted by the Johnston multipliers M1 and M3. The He^+ component was recorded as a current to F1 which was also used to calibrate the Johnston multipliers M1 and M3 *in situ* by the use of He^+ beams of very low intensity.

2.2. *Measurement procedure and signal analysis*

For the measurements of total cross sections $\sigma(He^{2+})$ for He^{2+} formation, both He^+ beams were modulated in a carefully programmed sequence of pulses (Mitchell *et al* 1977). This allowed the required He^{2+} signal from the collision processes of interest to be distinguished from that arising from collisions with the background gas. Absolute cross sections $\sigma(He^{2+})$ could then be obtained from the relation

$$\sigma(\mathrm{He}^{2+})=\frac{Se^2v_1v_2}{(v_1^2+v_2^2)^{1/2}}\cdot\frac{F}{I_1I_2} \tag{5}$$

where S is the He^{2+} count rate after allowing for the measured efficiency of detection; I_1, I_2 and v_1 and v_2 are the currents and velocities of the projectile and target beams respectively. The form factor F, which is a measure of the overlap of the two beams, was determined (as in our previous work) by carrying out a profile scan of each beam. The moveable slits required to do this are not shown in figure 1. In a typical measurement at a CM energy of 179 keV, a fast He^+ beam of 10.6×10^{-6} A collided with an 8 keV He^+ beam of 0.53×10^{-6} A. The resulting signal S was 282 counts/s while the background count rate was 2003 counts/s.

At each CM energy, careful checks were carried out to ensure that cross sections $\sigma(He^{2+})$ derived from (5) were independent of beam intensities and profiles so that S

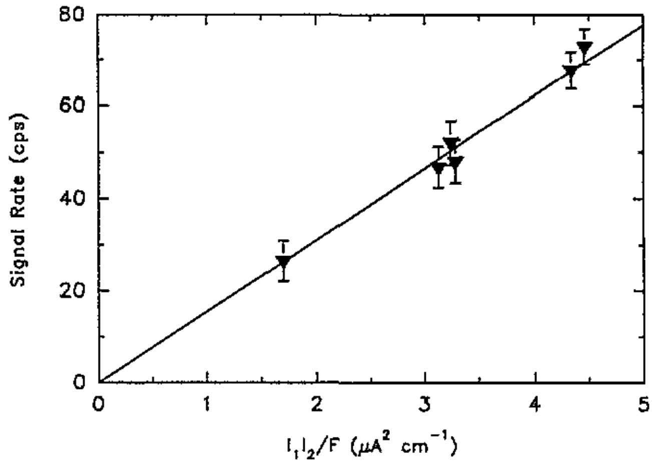

Figure 2. Dependence of He^{2+} product signal count rate on product I_1I_2/F (see text).

was linearly dependent on the product I_1I_2/F. Figure 2 shows a typical plot obtained at a CM energy of 154 keV. A number of additional checks were also carried out (cf Neill *et al* 1982) to ensure that the angular acceptance of M2 was large enough to accommodate all the scattered He^{2+} products.

For the measurements of the cross sections ${}_{11}\sigma_{02}$ for charge transfer and ${}_{11}\sigma_{22}$ for simultaneous electron loss by both He^+ ions, neither of the beams was modulated and a coincidence counting technique was used. In the case of ${}_{11}\sigma_{02}$, the He^{2+} pulses from M2 provided the start signals for a time-to-amplitude converter (TAC) while the He atom signal from M1 after an appropriate delay provided the stop signals. Output pulses from the TAC were then recorded by a multichannel analyser where the He^{2+}–He coincidence signal could be distinguished above the random background. In a typical measurement, where a 350 keV He^+ beam of 5.95×10^{-8} A collided with an 8 keV He^+ beam of 6.83×10^{-7} A, a coincidence signal of 0.9 counts/s was recorded above the random background of 3.8 counts/s.

For the measurements of the cross sections ${}_{11}\sigma_{22}$ for simultaneous electron loss by both He^+ ions a similar arrangement was used in which the two He^{2+} products from the same collision were counted in coincidence using counters M2 and M3. It is also worth emphasising that, in the measurements of ${}_{11}\sigma_{02}$ and $\sigma(He^{2+})$, M2 rather than M3 was used since the background signal arising from electron loss by the target He^+ beam in the residual gas was considerably less than that associated with the higher energy projectile beam. The two-stage electrostatic analyser preceding M2 also ensured an improved signal/background ratio.

3. Results and discussion

Our measured absolute cross sections $\sigma(He^{2+})$ for He^{2+} production and ${}_{11}\sigma_{02}$ for charge transfer are shown in table 1. Cross sections ${}_{11}\sigma_{22}$ for simultaneous electron loss by both He^+ ions were found to be too small to measure accurately even at our highest energies; an upper limit of only 2×10^{-18} cm^2 was estimated for ${}_{11}\sigma_{22}$ at a CM energy of 229 keV. The contribution of ${}_{11}\sigma_{22}$ in equation (5) could therefore be ignored as

Table 1. Absolute cross sections $\sigma(He^{2+})$, ${}_{11}\sigma_{02}$ and ${}_{11}\sigma_{12}$ for He^{2+} production, charge transfer and ionization respectively in He^+–He^+ collisions. Only statistical uncertainties are shown at the 90% confidence level. All values of $\sigma(He^{2+})$, ${}_{11}\sigma_{02}$ and ${}_{11}\sigma_{12}$ are subject to respective estimated uncertainties of ±6.5%, ±9.3% and 11% in absolute magnitude due to systematic errors.

CM energy (keV)	$\sigma(He^{2+})$ ($cm^2 \times 10^{-18}$)	${}_{11}\sigma_{02}$ ($cm^2 \times 10^{-18}$)	${}_{11}\sigma_{12}$ ($cm^2 \times 10^{-18}$)
54	20.1 ± 1.3	—	—
79	27.8 ± 3.0	17.1 ± 2.7	10.2 ± 3.9
104	28.9 ± 1.5	18.1 ± 1.5	10.9 ± 2.1
129	29.3 ± 1.8	18.7 ± 1.5	10.6 ± 2.3
154	29.9 ± 1.5	15.7 ± 1.2	14.2 ± 2.0
179	32.1 ± 0.7	14.7 ± 0.9	17.4 ± 1.2
205	30.2 ± 1.1	12.5 ± 0.9	17.7 ± 1.5
229	27.2 ± 1.7	11.2 ± 1.3	16.0 ± 2.1

relatively small and the cross sections ${}_{11}\sigma_{12}$ for ionization included in table 1 were derived from the difference ${}_{11}\sigma_{12} = \sigma(He^{2+}) - {}_{11}\sigma_{02}$. The uncertainties associated with individual cross sections in table 1 represent 90% confidence limits based on the counting statistics. In addition, the absolute magnitudes of $\sigma(He^{2+})$, ${}_{11}\sigma_{02}$ and ${}_{11}\sigma_{12}$ are subject to estimated uncertainties of ±6.5%, ±9.3% and ±11% respectively due to systematic errors.

Our cross sections $\sigma(He^{2+})$ for He^{2+} production may be compared in figure 3 with the previous low energy measurements by Peart *et al* (1983) and by Melchert *et al* (1987a). At 100 keV, agreement with the results of the latter is excellent but our lowest energy cross section at 54 keV is only 84% of the values obtained in both the previous measurements.

In figure 4 our cross sections ${}_{11}\sigma_{02}$ for charge transfer may be compared with the previous measurements and with a number of theoretical predictions. The cross sections previously measured by Melchert *et al* attain a peak value at a CM energy of about 55 keV and then decrease steadily with increasing energy to their 112 keV energy limit. This high energy trend is not confirmed by the present values of ${}_{11}\sigma_{02}$ which increase

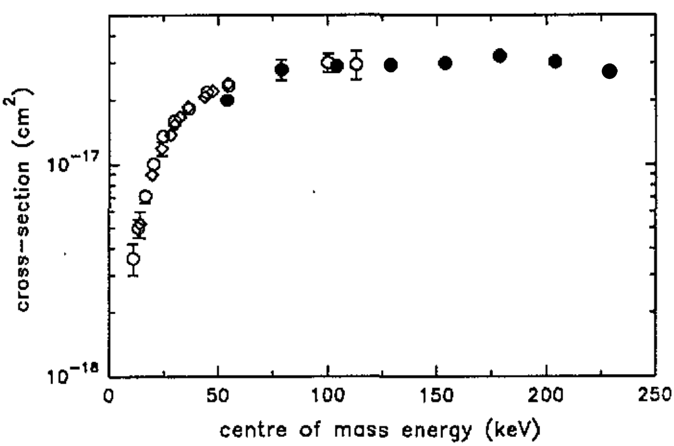

Figure 3. Total cross sections $\sigma(He^{2+})$ for He^{2+} production in He^+–He^+ collisions. ●, present results; ○, Melchert *et al* (1987a); ◇, Peart *et al* (1983).

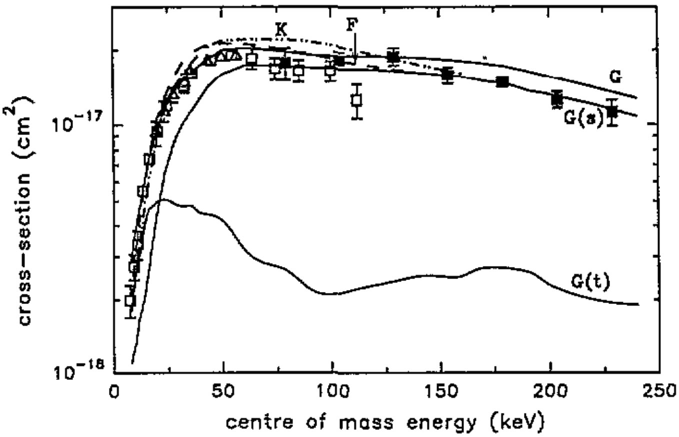

Figure 4. Cross sections ${}_{11}\sigma_{02}$ for charge transfer in He^+–He^+ collisions. Experimental data: ■, present results; □, Melchert *et al* (1987b); △, Peart *et al* (1983). Theory: curve G, Gramlich *et al* (1989) (curves G(t) and G(s) are the respective contributions for electron capture into triplet and singlet states only); curve K, Kimura (1988); curve F, Fritsch and Lin (1987).

from our low energy limit of 79 keV, attain a peak near 129 keV and then exhibit a decrease with increasing energy. Although it could be argued that the agreement between our two lowest energy values of ${}_{11}\sigma_{02}$ at CM energies of 79 keV and 104 keV and the results of Melchert *et al* (1987b) is within the maximum combined experimental uncertainties, the high energy trend of the two sets of data is quite different. Indeed, at 112 keV, corresponding to the highest energy datum point of Melchert *et al* (1987b), our interpolated value of ${}_{11}\sigma_{02}$ is about 1.5 times larger than their value. If we ignore the 112 keV datum point of Melchert *et al* (1987b) the two sets of experimental data indicate an unusually broad peak in the energy dependence of ${}_{11}\sigma_{02}$. Indeed there is some evidence of the double peak structure predicted by the calculations of Gramlich *et al* (1989) based on a coupled state approach with Gauss type orbitals. These calculations, while in reasonably good general accord with the observed broad structure of ${}_{11}\sigma_{02}$, predict high energy values which are too large. The calculations of Gramlich *et al* (1989) also indicate that electron capture into triplet states provides the dominant contribution to ${}_{11}\sigma_{02}$ at CM energies below 20 keV. However at higher energies, their calculations predict that electron capture into singlet states is dominant. The predicted singlet and triplet contributions are included in figure 4.

Kimura (1988) has used a travelling molecular orbital method within a semiclassical formalism to predict values of ${}_{11}\sigma_{02}$ in the CM range 10–160 keV. These can be seen (figure 4) to provide a reasonable description of our measurements above about 120 keV and the measurements of both Peart *et al* (1983) and Melchert *et al* (1987b) below about 30 keV. These calculated values are larger than experiment at intermediate energies. Calculations by Fritsch and Lin (1987) in the CM energy range 8–140 keV based on an atomic orbital expansion method can be seen to be in slightly better accord with experiment at intermediate energies.

In figure 5 our derived cross sections ${}_{11}\sigma_{12}$ for ionization are shown together with the previous low energy measurements of Melchert *et al* (1987a). Although our values are somewhat smaller in the energy range of overlap, the agreement between the two sets of data is well within the maximum combined experimental uncertainties. Cross

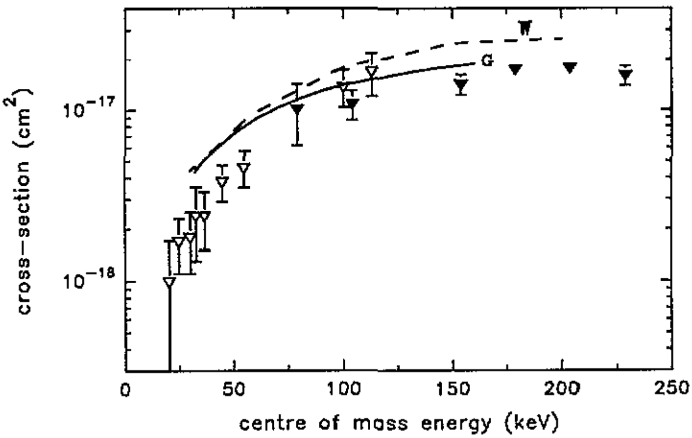

Figure 5. Cross sections ${}_{11}\sigma_{12}$ for ionization in He^+-He^+ collisions. Experimental data: ▼, present results; ∇, Melchert *et al* (1987a). Theory: curve G, Gramlich *et al* (1989); curve W, Willis *et al* (1985).

sections ${}_{11}\sigma_{12}$ calculated by Willis *et al* (1985) using a classical-trajectory Monte-Carlo method and by Gramlich *et al* (1989) using the coupled states method (figure 5), while larger, do reproduce the energy dependence of the experimental data reasonably well.

4. Conclusion

The present experimental studies of He^+-He^+ collisions in the CM energy 54–229 keV provide a useful extension of previous low energy measurements. We have shown that both charge transfer and ionization make important contributions to He^{2+} production in the energy range considered while the process of simultaneous electron loss by both He^+ ions is relatively unimportant. While agreement with previous low energy measurements is generally satisfactory, some discrepancies have also been noted. In particular, the present cross sections ${}_{11}\sigma_{02}$ for charge transfer indicate an unusually broad structure similar to that predicted by the calculation of Gramlich *et al* (1989).

Acknowledgments

This work is part of a programme supported by a Rolling Grant from the Science and Engineering Research Council. One of us (JGM) is also indebted to the Department of Education, Northern Ireland for the award of a Research Studentship.

References

Fritsch W and Lin C D 1987 *Phys. Lett* **123A** 128
Gilbody H B 1982 *Physics of Electronic and Atomic Collisions* ed S Datz (Amsterdam: North-Holland) p 223
Gramlich K, Grün N and Scheid W 1989 *J. Phys. B: At. Mol. Opt. Phys.* **22** 2567
Kimura M 1988 *J. Phys. B: At. Mol. Opt. Phys.* **21** L19

Melchert F, Rink K, Rinn K and Salzborn E and Grün N 1987a *J. Phys. B: At. Mol. Phys.* **20** L223
Melchert F, Rink K, Rinn K and Salzborn E 1987b *J. Phys. B: At. Mol. Phys.* **20** L797
Mitchell J B A, Dunn K F, Angel G C, Browning R and Gilbody H B 1977 *J. Phys. B: At. Mol. Phys.* **10** 1897
Neill P A, Angel G C, Dunn K F and Gilbody H B 1982 *J. Phys. B: At. Mol. Phys.* **15** 4219
Peart B, Rinn K and Dolder K 1983 *J. Phys. B: At. Mol. Phys.* **16** 2831
Salzborn E 1989 *J. Physique Colloque* C1 (Suppl. 1) **50** 207
Willis S L, Peach G, McDowell M R C and Banerji J 1985 *J. Phys. B: At. Mol. Phys.* **18** 3939